The climatological annual cycle of satellite-derived phytoplankton pigments in the Alboran sea: a physical interpretation

E. Garcia-Gorriz, M.-E. Carr

Jet Propulsion Laboratory/Caltech, Pasadena, CA

Corresponding author address: E. Garcia-Gorriz, Jet Propulsion Laboratory/Caltech, MS-300/323, 4800 Oak Grove Dr., Pasadena, CA 91109. E-mail: eg@pacific.jpl.nasa.gov

Abstract

The circulation and upwelling processes (coastal and gyre-induced) that control the **phytoplankton distribution** in the **Alboran sea** are examined by analyzing monthly climatological patterns of Coastal Zone Color Scanner (CZCS) pigment concentrations, sea surface temperatures, winds, and seasonal geostrophic fields. We will also consider Sea-viewing Wide Field-of-view Sensor (SeaWiFs) and Ocean Color and Temperature Scanner (OCTS) color data, and available in situ data. The Alboran sea presents two climatological states: a fall-to-winter bloom (November-March) and a non-bloom period (May-September). The role of the physical forcing due to upwelling and circulation patterns on the evolution and distribution of pigment concentrations, and the interaction between **coastal upwelling** and **circulation** are discussed.

Introduction

Although the Western Mediterranean sea is generally oligotrophic, the Alboran sea reaches relatively high surface concentrations of pigments throughout the year. This western-most Mediterranean basin serve as a transition between the Atlantic Ocean and the Mediterranean Sea, which are connected through the Strait of Gibraltar. The Alboran sea presents within its small area the major processes of physical-biological interaction seen in the ocean. Fig. 1 shows the geographical location of the Alboran sea and our four sub-areas of study: Atlan (the eastern Atlantic Ocean in the vicinity of the Strait of Gibraltar), Alb (the entire Alboran sea), Wgyre (western Alboran basin) and Upwell (a small area characterized by upwelling off the Spanish coast, in the northwest Alboran sea).

The circulation pattern in the Alboran sea presents two quasi-permanent anticyclonic gyres which almost cover the entire basin. The Atlantic influx overlies the Mediterranean water, which outpours into the Atlantic Ocean. The formation, mean position, intensity and shape of this

anticyclonic system is mainly ruled by the coexistence and mixing of Atlantic and Mediterranean waters, variations in the mass flux through the Strait of Gibraltar, topography, the effect of the Earth's rotation, and winds [Heburn and LaViolette, 1990]. The annual cycle of the spatial pattern of pigments in the Alboran sea is shaped by this circulation path and by the vertical supply of nutrients.

Two different types of upwelling occur in the Alboran sea: wind-induced coastal and eddy-induced upwelling associated with the anticyclonic gyres. The horizontal and vertical flux of nutrients into the euphotic zone results in the high observed chlorophyll concentration (Fig. 2a,b).

The objective of this paper is to study how the physics control the phytoplankton distribution in the Alboran sea throughout the year by examining monthly climatological averages of pigment concentration, sea surface temperature and wind, and seasonal geostrophic velocity within the basin. We will also consider SeaWiFs and OCTS color data for specific months, and other available in situ data.

Data:

We examine the monthly climatologies of the CZCS pigment distributions (CZCS-Chl hereinafter), the NOAA/NASA Advanced Very High Resolution Radiometer (AVHRR) sea surface temperature (SST hereinafter), and the European Remote Sensing Satellite (ERS-1) winds. The time span and spatial resolution of these data sets are the following: CZCS-Chl (1978-86, 19 km), SST (1985-95, 9 km), and ERS1 scatterometer winds (1992-95, 1°). Each of the climatologies has been computed as the arithmetic average of all pixels containing valid data for each one of the available months from several-year-long data sets. Therefore, they can be considered representative of the monthly physical-biological patterns within the Alboran sea inasmuch the periods were typical. The individual monthly fields for the time coverage of the three data sets will be also used, together with monthly SeaWiFs (10/97-5/98, 9 km), OCTS (11/96-6/97, 9 km) monthly images, and the multichannel sea surface temperature (MCSST) monthly averages (10/97-5/98, 19 km). We also examine the in situ seasonal climatologies of geostrophic currents computed by the Mediterranean Oceanographic Data Base (Univ. of Liege, Belgium). Their nominal resolution is 0.2° and they correspond to a depth of 5 m. The cruises from which these velocities were calculated took place from the 50s to the present.

Results

We start our cycle of CZCS-Chl in October, after the annual minimum in September (0.18 mg/m^3). From October, the mean value (0.31 mg/m^3) increases towards the winter season, when maximum values occur between December and February (Fig. 2a). The pigment concentration in Wgyre is higher than in the rest of Alb throughout the year. Local maxima of CZCS-Chl occur in February (1.91 mg/m^3) although the monthly mean is maximum in December (0.70, while 0.67 mg/m^3 in February). In April (not shown), the mean CZCS-Chl is almost half (0.38 mg/m^3) that of December, and monthly means decrease thereafter. From May to September, the pigment concentration is low in the Alboran basin: 0.3 for May and 0.21 mg/m^3 for June, July and August. The highest values are located in the coastal areas of western Alboran (north and south), and in the periphery of the western Alboran gyre. This pattern in pigment concentration allows the visualization of the Alboran gyres. From June to August, only the western gyre is unambiguously traced. And it is hardly visible in September and February, when the lowest and highest local values of the CZCS-Chl occur respectively.

Monthly CZCS data from individual years (not shown here) confirm that the maximum values of pigment concentration happen within the interval between November and February from 1982 to 86. They reach 6.0 in December 82 and 7.4 mg/m^3 in January 83, although in remaining years the maximum is close to 2 mg/m^3 within the December-February period. Exceptionally, year 79 displays a peak of 2.1 mg/m^3 in January accompanied by a slightly higher peak (2.3 mg/m^3) in July. The temporal pattern of CZCS-Chl values in Atlan is analogous to Alb.

When the SeaWiFs monthly images from 10/97 to 5/98 (Fig. 2b) and the CZCS climatologies (Fig. 2a) are compared, the trend of increasing concentrations until January, observed in CZCS, is also seen. However, the decreasing trend starts in February and is interrupted by high values in April 98. The pigment distribution in May 98 is very similar to the CZCS May distribution.

The SST climatologies reveal that three thermal regimes occur for the domain Atlan+Alb (Fig. 2c), where each image has its independent color-scale bar of temperatures to enhance the visual contrast of the SST patterns and to facilitate the detection of the circulation features which are correlated with the thermal signature . The three SST regimes are: (1) SST(Atlan)>SST(Alb) from November to April, (2) SST(Atlan)≈SST(Alb) in May, June and October, and (3) SST(Atlan)<SST(Alb) from July to September. The regimes occur because the Alb area reaches more extreme SST values than the Atlan in winter (14.2 and 15.1°C in February, respectively) and summer (25 and 23.5°C in August). When the individual monthly SST images within 1985-

95 are examined, the maximum values for Alb and Atlan fulfill the regimes described above except for the summer of 87 and 93, when both reach similar temperatures.

The direction and magnitude of the wind fields varies from month to month in the Alboran sea (Fig. 2a). The strongest winds are observed in January, May, and June. The periphery of the western Alboran gyre presents the same wind direction in May, June, August, and September. This wind pattern in the northern border of the gyre is conducive to coastal upwelling off the Spanish coast. The coarse spatial resolution of the satellite wind fields gives poor information about the actual wind regime in the center of the Alboran basin. However, there is a grid point with observations of the wind velocities in the northwest Alboran basin, where the Upwell area is located in Fig. 1. The Upwell area corresponds to a square of 0.2° of side and centered at [36.5 N, 4.5 W]. Westerly winds favor the occurrence of upwelling in May, June and August to November. May and June correspond to the maximum values with 8 and 10.5 m/s (Fig. 3a). The rest of the months have either downwelling or the wind alongshore is almost zero. Furthermore, the variability of the u-component of the wind is minimum from May to August and in January (Fig. 3b). It is maximum in April, September, October and December (Fig. 3b). The plots of SST and CZCS-Chl are out of phase in Upwell (Fig. 3a), as expected for upwelling nutrient-rich cold water leading to increased pigment concentrations. The maximum variability of the pigment concentration occurs from December to April (Fig. 3d).

We computed the correlation of the monthly horizontal patterns of SST and CZCS-Chl for both Alb and Wgyre. Normalized intervals of variation of the horizontal fields are considered to calculate the correlation. The SST and CZCS-Chl values are rescaled such that they vary within the zero-centered interval [-1,1] following the equation:

$$v_{res} = [v_{orig} - (\max(v_{orig}) - \min(v_{orig}))/2] \,/\, [\max(v_{orig}) - \min(v_{orig})] \quad (4),$$

where max and min indicate the maximum and minimum values of the original field v_{orig}, and v_{res} is the resulting field. The correlation between CZCS-Chl and SST fields is favourable when it is negative. The goal of equation (4) is to produce adimensional monthly fields (of CZCS-Chl and SST) which horizontal patterns are preserved but which variations are happening within the same interval. While the intervals of variation for CZCS-Chl are approximately common for each monthly distribution (Fig. 2a), the ones for SST have poor overlapping throughout the year. For example: in January and August, the intervals are 15- 17.5°C and 22- 25.5°C and any direct calculation of correlations becomes difficult. For the Alb area, the correlation drops from January to March (Fig. 4). From April to June, it increases in sinchrony with the increase of SST. It has a

local minimum when SST is maximum. The annual maximum is in October, and decreases from November to March.

Two data sets of in situ salinity and temperature also contribute to our study. Fig. 5 (a-f) shows the horizontal (at depth 6 m) and vertical profiles of two north-south CTD sampling transects. They correspond to two different cruises: the first held in April 86 and the second in September 92. The horizontal contour of salinity on April 96 reveals that Mediterranean water (salinity 38) is upwelling in the northwest of Wgyre and being carried away in the edge of the fresher Atlantic inflow (Fig. 5a). For September 92, there is no trace of upwelling (Fig. 5b). The Atlantic influx is easily identified in the vertical plot of salinity, while the temperature profile displays strong stratification in September 92. While the Atlantic inflow is significantly warmer in April [corresponding to thermal regime (1)], the isotherms dome upward in September [regime (3)].

From the geostrophic fields (Fig. 6a-d), winter and summer present a clear signature of a totally developed gyre. The shape of the eastern gyre is less visible. The maximum geostrophic velocities occur in summer. On the other hand, spring and fall fields display hints of both gyres, although with weaker currents. Spring velocities (and also in the fall to a lesser extent) suggest that the position for the center of the western gyre is shifted to a more southwestern location, closer to the coast of Morocco.

Discussion and Conclusions.

From the CZCS images (Fig. 2a), the temporal evolution of the pigment concentration throughout the year in the Alboran sea has two climatological states: the bloom period from November to March (fall-to-winter), and the non-bloom period from May to September. October-November and April-May are transition months between both. The scatterogram of (pigment, temperature) supports these scenarios and the pairs (CZCS-Chl, SST), (SeaWiFs-Chl, MCSST), and (OCTS-Chl, MCSST) in Fig. 7 reveal that the monthly values for Wgyre lie within a (pigment, temperature) band. The area covered by this band is centered by a four-degree polynomial, which fits the (CZCS-Chl, SST) values via least-squares. The dashed lines in Fig. 7 comprises all observations (calculated from the polynomial ±1 std of CZCS-Chl). The bloom occurs for temperatures smaller than ~17.4°, while the non-bloom period begins for temperatures above ~19.5°. The November and May values have temperatures between this scenarios, and their pigment and SST distributions are significantly different from each other: bloom and non-bloom

respectively (Fig. 2a). The (CZCS-Chl, SST) slope is greatest in the bloom period and least in the transition between bloom and non-bloom.

The SeaWiFs pigment distributions in October 97 illustrates the control of temperature over the transition toward the bloom period. From 10/97 to 5/98 the temperatures were higher than typical. October 97 was 2°C warmer than the average (Fig. 7). We conclude that the typical September situation lasted during October 97 due to high temperatures. November 97 behaved as expected, but still about 1°C warmer. Finally, a warmer and poorer bloom occurred in winter 97-98. The OCTS points in Fig. 7 fall within the band area, although 11-12/96 and 1/97 are higher than typical.

The horizontal patterns of ocean color do not necessarily coincide with SST features since ocean color is dependent on complex interrelationships involving biological, chemical, and physical ocean processes [Arnone, 1987], while SST responds to circulation and air-sea interaction. However, in the Alboran sea, the presence of the gyres is visualized in both the CZCS-Chl and SST images for a number of months throughout the year (Fig. 2a,c). The horizontal correlation of SST and pigments is closely linked to the presence of the gyre signature (specially the western gyre), which is enhanced during the non-bloom period. From April to July, the correlation is steadily increased in agreement with the seasonal heating and the start of the stratification period. Concurrently, there are wind-induced cold upwelled waters in the northwest of the basin as seen in the SST images (Fig. 2c). These nutrient-rich upwelled waters favour local phytoplankton growth and contrast with the surrounding oligotrophy. Our climatological results are consistent for the bloom season with those presented by Morel and Andre [1991]: typical concentrations of 0.5 to more than 1 mg/m^3 circling inner cores, where surface pigments remain much lower (0.15-0.25 mg/m^3). For the non-bloom season, the value drop to 0.3-0.6 in the periphery and 0.1-0.2 mg/m^3 in the inner core.

Light does not seem to be a limiting-factor for phytoplankton growth throughout the year in the Alboran sea. The annual bloom has its maximum values during winter. This fall-to-winter bloom differs from the most significant blooms in other parts of the Western Mediterranean sea (like the Gulf of Lions), where the spring bloom is the annual maximum and there is a secondary bloom in fall.

When the late-spring strong winds blow alongshore the Spanish coast causing upwelling, the Atlantic influx has similar temperature to the water in Alb. It is non-bloom season. This coincidence favours the detection of cold water and its identification as resulting from upwelling

in the SST images. This cold upwelled water is partially advected by the western gyre towards the coast of Africa. Likewise, the periphery of the gyre presents upwelling velocities of $5x10^{-5}$ m/s (5 m/d) [Viudez et al., 1996] which also supply nutrients to the surface. The dynamics of the gyre (and in general, of mesoscale structures) can produce vertical motions that transport nutrients into the euphotic zone. The combined interaction of the coastal and gyre-induced upwelling with local dynamics control the sub-surface pigment distribution in the Alboran sea.

In consequence, the pigment concentration in the periphery of the gyre during the non-bloom season has two main contributions: that advected from the coastal-upwelling sites and that due to in situ growth. The tendency is mantained from May to August (even if July presents no upwelling-favourable winds in the coast). The SST images from July to September do not enable tracking of the cold upwelled water since the Atlantic inflow is cold compared to the Alboran sea temperature (regime (3) of SST). However, the gyre signature is identifiable in both SST and CZCS-Chl distributions. The area of coastal upwelling is locally inhibited in September by stratification to the pigment annual minimum (Fig. 2a). In warmer years, this situation can be maintained throughout October, as observed in the SeaWiFs image (Fig. 2b). The winds are favourable to upwelling but weak and we conclude that strong stratification prevents the coastal upwelling. Furthermore, this is confirmed by the horizontal and vertical profiles of in situ salinity and temperature for September 92 (Fig. 5 d,e and f). The lack of upwelling during the stratified season contrasts with the presence of cold Mediterranean waters in the sea surface (with salinities of 38) in April 86 (Fig. 5 a, b and c).

In October, the cold upwelled water is again visualized in the climatologies, since the temperature in both Atlan and Alb is approximately the same (regime (2) of SST). The October CZCS-Chl image shows an increase in the pigment concentration, and the correlation between SST and CZCS-Chl is maximum (Fig. 4) since the signature of the western gyre is visible in both distributions (Fig. 2a,c). Local Alb water starts to be convectively destratified in October (and November) and the SST isotherm pattern does not change much from December to April. The warm Atlantic influx can be detected in the east side of the Strait of Gibraltar in both the SST images and in the in situ vertical profile for April 86.

The three SST regimes for Atlan and Alb defined from the monthly climatologies are consistent with the results of Folkard et al. [1997]. They also found striking seasonal changes in the thermal nature of the surface inflow to the Alboran sea. Especially in winter to early spring, when the inflow retains a warm anomaly in the Wgyre, as seen from Dec to April in Fig. 2c. This

result differs from the classical definition of the Alboran sea as the first junction between the warm, highly saline waters of the Mediterranean and the colder, less-saline waters of the Atlantic given by LaViolette [1984]. This latter definition was consistent with SST data of the late summer of 1982 (analyzed by LaViolette [1984]).

The wind in the Upwell area (Fig. 3a) is either no upwelling-favourable or weak during bloom months (with November as an exception, Fig. 3a). The generally high concentration during the bloom months partially mask the local growth associated with coastal upwelling. During the transition month of April 86 cold nutrient-rich Mediterranean waters are observed in in situ data, but we cannot ascertain the presence of upwelling during the previous bloom months from the satellite observations. This coastal upwelling region (and the southern to a lesser extent) is the source of the nutrients of the Alboran sea during the non-bloom season. The drop of the CZCS-Chl curve at April-May in Upwell (Fig. 3a) would be much steeper, reaching values like those in the center of the gyre, if no wind-induced upwelling occurred.

Numerical models indicate that the narrowness of the Strait of Gibraltar and the angle with respect to the Alboran sea are regarded as significant causes for the shape, location and formation of the western Alboran gyre [Heburn and LaViolette, 1990]. From our seasonal climatological perspective, two dynamic situations are possible: the inflow at Gibraltar is directed to the northeast and the western gyre is fully formed (in winter and summer, Fig. 6a,c), or the inflow is directed eastward, and the gyre is substantially reduced in size and trapped against the Moroccan coast (in spring and fall, Fig. 6b,d). We suggest that the occurrence of this coastal upwelling in spring contributes (among other agents, such as variations in the Atlantic inflow, for example) to the southwest migration of the western gyre as well as to the reverse migration in summer (while inhibition of upwelling by stratification is occurring). Fall geostrophic fields would suggest that upwelling occurs even as the cooling season advances and CZCS images show high pigments close to the coast. During the fall-to-winter bloom, coastal areas are richer in pigments than the central locations in the basin. However, we cannot track upwelled water from our images (we have no in situ data available for this season) and the winds are not upwelling-favorable. As the winter geostrophic field suggest, upwelling may be weak or masked by the bloom conditions.

As a continuation of this study, we will explore the interplay of dynamics and circulation with local growth with the help of a numerical model forced by realistic winds and satellite images for both the bloom and non-bloom periods to assess phytoplankton growth in the periphery of the gyre due to advected upwelled waters vs. the local growth induced by the gyre.

Acknowledgments. The authors thank David Halpern, Peter Woisceshyn, and Kelly Perry for providing the ERS-1 data and the NOAA/NASA AVHRR Pathfinder project for providing daily sea-surface temperature via JPL-PODAAC. The National Space Development Agency of Japan (NASDA) retains ownership of the OCTS (ADEOS) data. NASDA supports the authors in acquiring the satellite data at a marginal cost. E.G.-G. research is funded by the National Research Council and the NASA Ocean Biogeochemistry Program and M.-E.C. by the NASA Ocean Biogeochemistry Program.

References

Arnone, R.A., Satellite-derived color-temperature relationship in the Alboran sea. Remot. Sen. Environ., 23, 417437, 1987.

Arnone, R.A., P.E. LaViolette, Bio-optical variability in the Alboran sea as assessed by Nimbus 7 Coastal Zone Color Scanner, NORDA, NSTL, MS, NTN, 283pp, 1984.

Arnone, R.A., The temporal and spatial variability of Chlorophyll in the Western Mediterranean. Coastal and Estuarine Studies. Seasonal and Interannual Variability of the Western Mediterranean Sea.Editor: P.E. LaViolette. AGU, 1985.

Folkard, A.M., P.A. Davies, A.F.G. Fiuza, I. Ambar, Remotely sensed sea surface thermal patterns in the Gulf of Cadiz and the Strait of Gibraltar: variability, correlations, and relationships with the surface wind field, J. Geophys. Res, 102 (3), 5669-5683, 1997.

Heburn, G.W., P. E. LaViolette, Variations in the structure of the anticyclonic gyres found in the Alboran sea, J. Geophys. Res., 95 (2), 1599-1613, 1990.

LaViolette, P.E., The advection of submesoscale thermal features in the Alboran sea gyre, JPO,14, 555-565, 1984.

Morel, A., J-M. Andre, Pigment distribution and primary production in the Western Mediterranean as derived and modeled from Coastal Zone Color Scanner observations, J. Geophys. Res., 96(7), 12685-12698, 1991.

FIGURES

Figure 1:

a) Location of the Alboran basin within the Western Mediterranean sea.

b) Subareas of study: Alb (Alboran sea), Wgyre (western Alboran basin), Atlan (Atlantic Ocean in the vicinity of the Strait of Gibraltar), and Upwell (a squared area in the coastal upwelling area).

Figure 2:

a) CZCS monthly climatological pigment distributions for October, November, December, February, May, July, August and September. The ERS-1 monthly winds are also plotted.

b) SeaWiFs monthly distributions from 10/97 to 6/98. These plots share the colorbar with Fig. 2a.

c) Same months as in Fig. 2a but for climatological SST.

Figure 3: a) SST (°C), Upwelling favorable (alongshore) wind u-component (m/s), and CZCS pigment concentration (*10 in mg/m^3) in the Upwell area.

b) Std of the Upwelling favorable wind component (m/s) in Upwell.

c) Std of the SST (°C) in Upwell.

d) Std of CZCS pigment concentration ($10*mg/m^3$) in Upwell.

Figure 4: Correlation between SST and CZCS-Chl (star)- the left y-axis has favorable correlations upward-, SST maximum values for Alb (circle) and Atlan (triangle) in °C.

Figure 5: a) Salinity contour at 6 m for April 86 (transect for vertical profiles is marked with circles)

b) Vertical profile of salinity along the transect for April 86.

c) Vertical profile of temperature along the transect for April 86.

d) Same as a) but for September 92.

e) Same as b) but for September 92.

f) Same as c) but for September 92.

Figure 6: Seasonal climatologies of the geostrophic velocity fields at 5 m: winter (a), spring (b), summer (c) and fall (d).

Figure 7: Scatterogram of pigment concentration and sea surface temperature for [CZCS-Chl, SST] (large), [SeaWiFs-Chl, MCSST] (medium), and [OCTS-Chl, MCSST] (small) in the Wgyre area. The numbers in the plot locate the value for this month of the year. The error-bars are the std of the pigment values for each month. The thick line plots the four-degree polynomial which fits the climatology points [CZCS-Chl, SST] in Wgyre. The dashed lines are the polynomial ±1 std of the CZCS-Chl (also in the Wgyre). The thick horizontal lines indicate the approximate dividing temperature between the bloom and non-bloom climatological regimes.

FIGURE 1

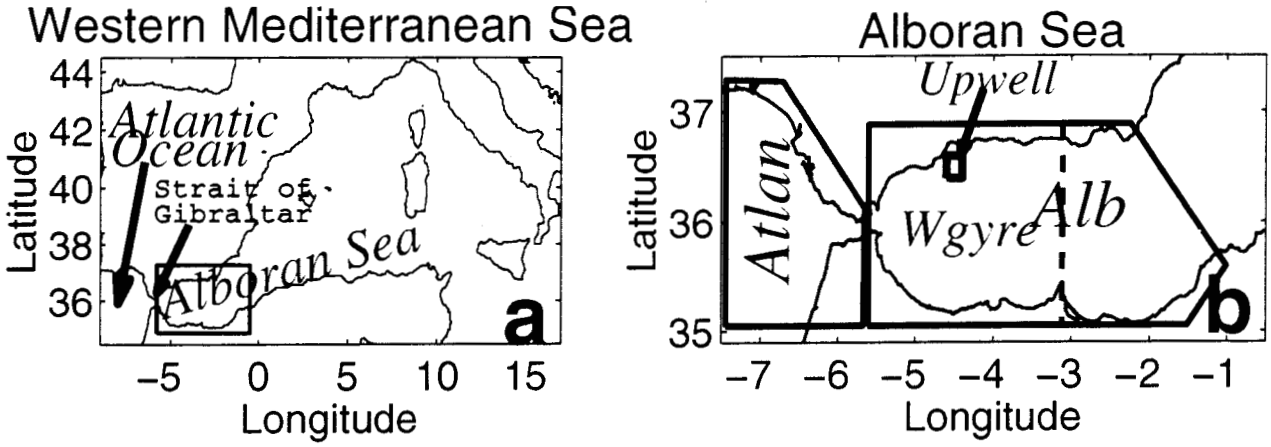

FIGURE 2a

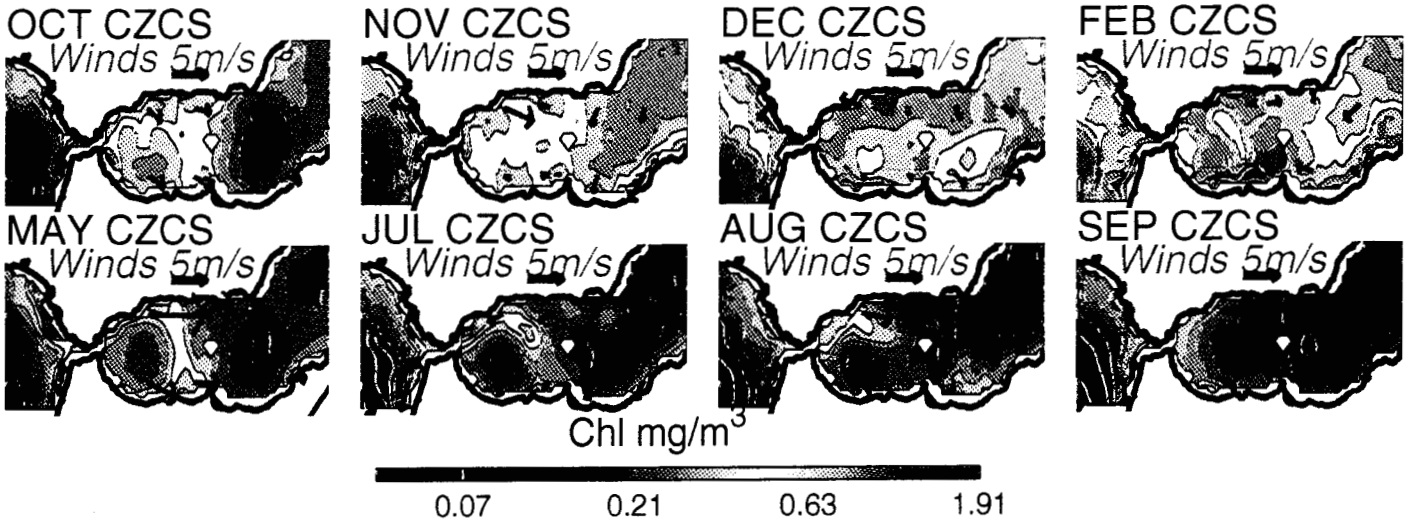

FIGURE 2b

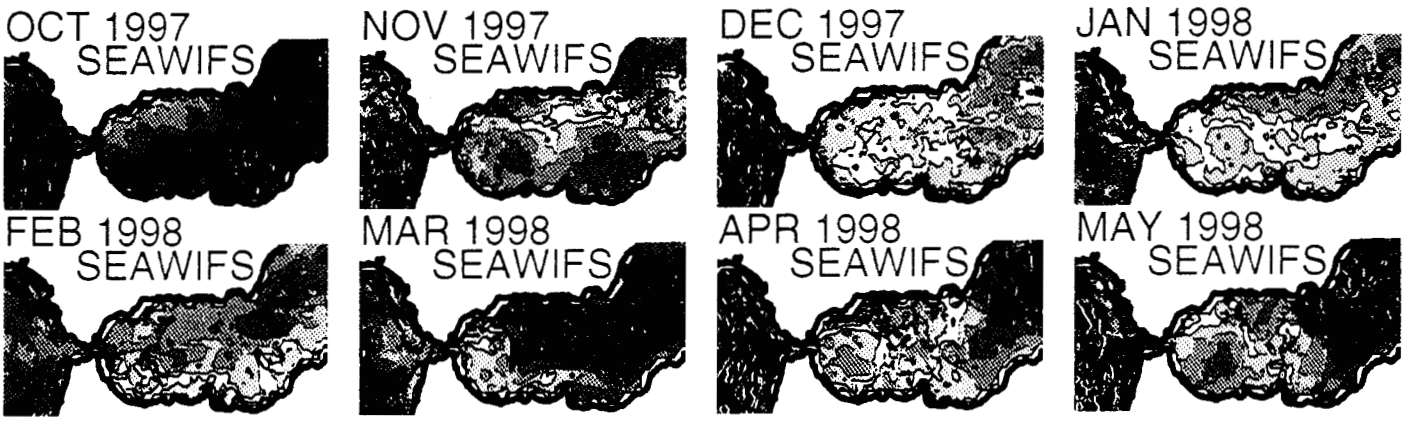

FIGURE 2c

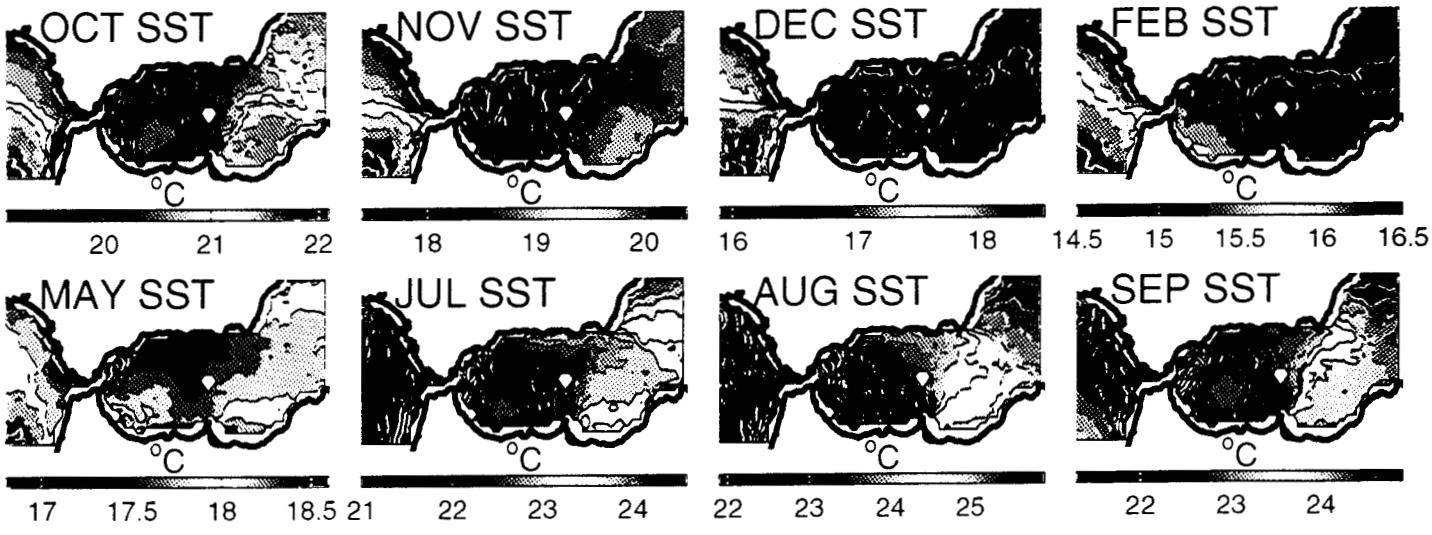

FIGURE 3

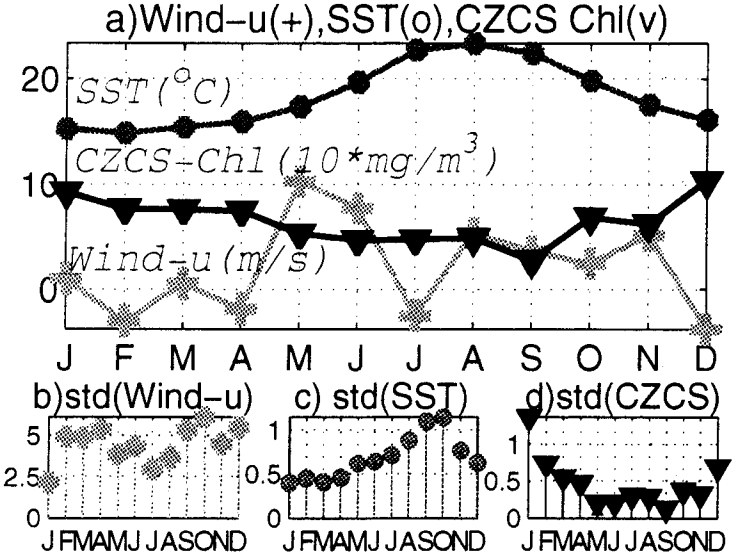

FIGURE 4

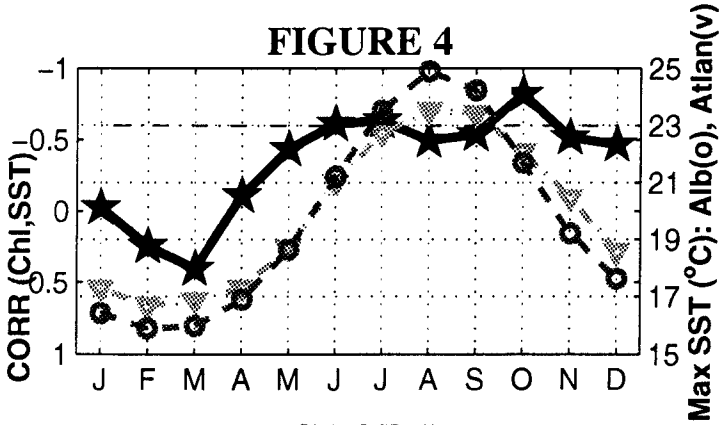

FIGURE 5

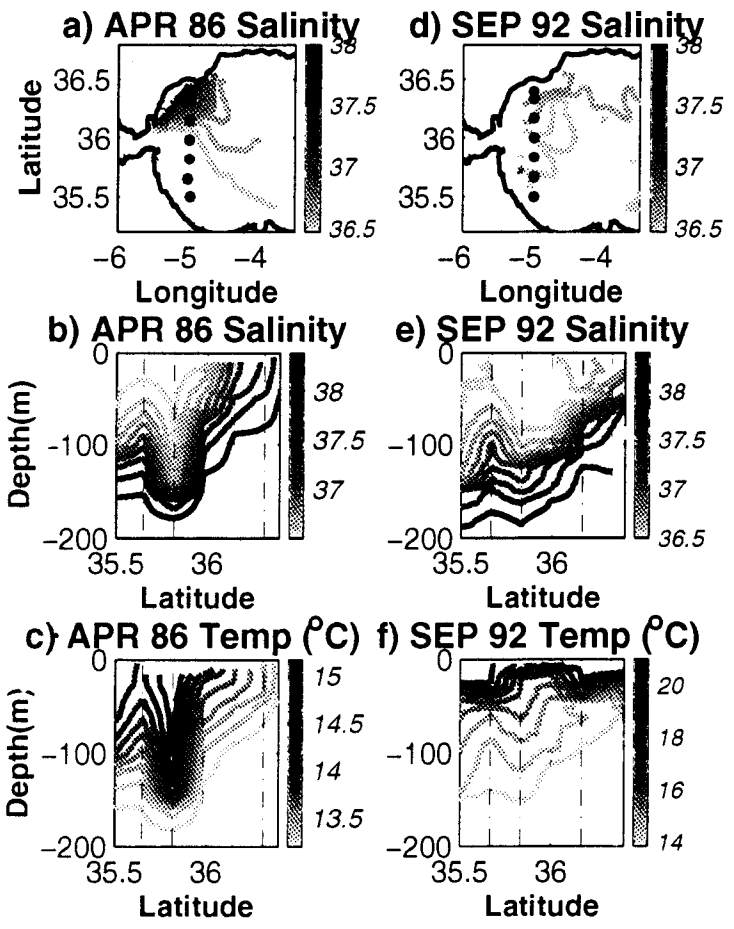

FIGURE 6

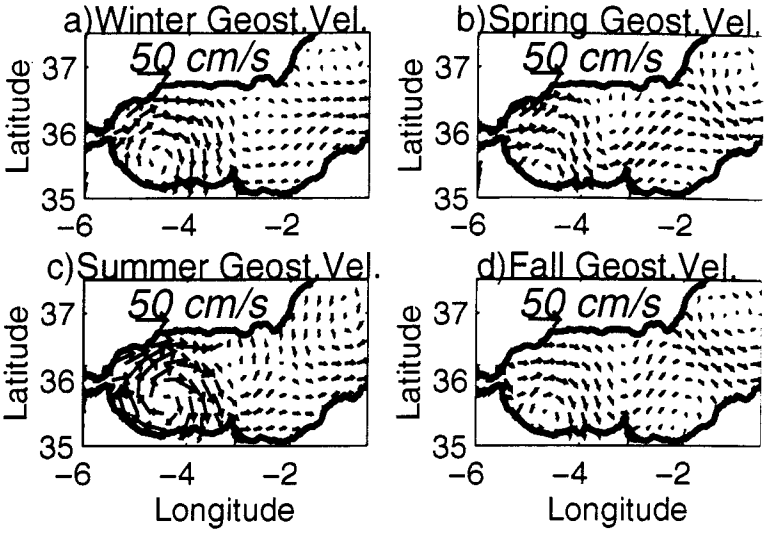

FIGURE 7